Journal of Innovation and Development
ISSN: 2958-4752 | Vol. 8, No. 2, 2024

Research on the Pass Capacity Model of Logging Tools for Complex Horizontal Wells

Hongyun Zhang [1, *], Jibin Zhong [2], Hao Zhang [3], Xindi Zhao [1], Lvyin Lei [3]

[1] China Petroleum Logging Co., Ltd. Southwest Branch, Chongqing, 401139, China
[2] China National Petroleum Corporation, Changqing Oilfield Company, Xi'an Shaanxi, 710000, China
[3] China Petroleum Logging Co., Ltd, Xi'an Shaanxi, 710054, China

*** Corresponding author:** Hongyun Zhang

Abstract: Shale gas, which exists in organic-rich shale or mud shale formations primarily in adsorbed or free states, poses significant development challenges due to the low permeability of shale formations. Traditional vertical wells are ineffective for shale gas extraction, making horizontal wells and large-scale hydraulic fracturing essential for efficient development. However, the complexity of the formation can lead to casing deformation, severely impacting the pass capacity of plug and perforation gun strings in the wellbore. This study analyzes the causes of casing deformation and discusses the rapid development of the cluster perforating technology in perforation operations, and discusses the challenges that might encountered during the process of wireline conveying or pumping. The irregular trajectory of horizontal wells and the high dogleg deflecting severity in the deviated sections can cause cluster perforating strings to suddenly get stuck during the downhole process, leading to a sudden increase in pumping pressure, which may result in premature seating of the fracturing bridge plug, or pull-off accidents at the weak point of the wireline. This research aims to improve engineering efficiency and prevent engineering accidents by conducting a pass capacity analysis of the perforating tool string, which is of significant engineering importance for shale gas development.

Keywords: Shale Gas Development; Casing Deformation; Horizontal Wells; Cluster Perforating; Wireline Conveyance; Pass Capacity Analysis.

1. Introduction

The development of shale gas is crucial for meeting the global energy demand, particularly within formations rich in organic matter. However, the low permeability of these strata, where shale gas primarily exists in adsorbed or free states, poses significant challenges to extraction efforts. To effectively tap into these resources, the industry commonly employs horizontal well and large-scale hydraulic fracturing technologies. While these methods have addressed permeability issues to some extent, the complexity of the geological formations often leads to casing deformation before the perforation tools are run in, which not only affects the pass capacity of plug and perforation gun strings in the wellbore but also increases operational risks.

Casing deformation is a complex phenomenon influenced by multiple factors. Analysis of data from several measured wells has revealed that the main causes of casing deformation include changes in the geostressed field, formation deformation, slippage of natural fractures, defects in cementing quality, and asymmetry in the fractured area. The combined effect of these factors or the cumulative impact of certain minor factors can lead to casing deformation.

Numerous scholars have conducted extensive research on the pass capacity of downhole tools in horizontal wells and casing deformation issues. Starting from the calculation method for the pass capacity of downhole tools in high-angle wells under the condition of ignoring tool string deformation proposed by Ran Jing et al. in 1990, to the through model for medium and short-radius deviated drilling tools in horizontal wells established by Chen Zushi et al. in 1999, to the length control equation for cluster perforating coiled tubing strings under rigid conditions in horizontal wells established by Zhu Xiuxing et al. in 2013, and the geometric method used by Luo Quan et al. in 2014 to analyze the pass capacity of downhole tools, these studies have provided important theoretical foundations for understanding the pass capacity of downhole tools.

In terms of research on casing deformation mechanisms, Yang Long conducted in-depth research on casing failure mechanisms in 2003, Liu Wei et al. conducted numerical simulation studies on the deformation and failure mechanisms of casings in tight oil reservoir horizontal wells during volume fracturing in 2017, Guo Xue Li et al. studied the deformation mechanism of casings in shale gas fracturing wells based on seismogenic mechanisms in 2018, and Chen Chao Wei et al. conducted a detailed analysis of casing deformation characteristics in Sichuan shale gas wells in 2021. These studies have not only enriched our understanding of casing deformation but also provided a scientific basis for its prevention and treatment.

This paper aims to synthesize previous research findings, conduct a systematic analysis of the pass capacity of downhole tools in horizontal wells and casing deformation issues, explore their influencing factors, and propose corresponding preventive and improvement measures, in order to provide theoretical and technical support for the safe and efficient development of shale gas.

2. Investigation of the Pass Capacity Model for Logging Tool Strings

2.1. Wellbore Trajectory Simulation

Wellbore trajectory analysis is a key technology in petroleum engineering, involving the description and simulation of the three-dimensional spatial curve formed during the drilling of horizontal wells. In petroleum engineering practice, the wellbore trajectory is a spatial curve

obtained by connecting a series of survey points obtained from logging using geometric methods. Different wellbore trajectory simulation methods have certain errors compared to the actual wellbore trajectory, and these errors can significantly affect the accuracy of subsequent work. The survey point data usually include parameters such as inclination angle, azimuth, well depth, and dogleg severity, and the wellbore trajectory is formed by processing and fitting these data. The trajectory can be described using two coordinate systems: the natural coordinate system and the spatial rectangular coordinate system.

The three-dimensional wellbore methods used for wellbore trajectory simulation mainly include the slice method, minimum curvature method, cylindrical helix interpolation method, cubic spline interpolation, and polynomial fitting smoothing method. Among them, the cubic spline function interpolation method is used for wellbore trajectory simulation, which can determine the inclination angle and azimuth at any point between two known survey points. This calculation method is simple, stable, convergent, has high simulation accuracy, and the wellbore trajectory curve is continuous and smooth. Therefore, this paper uses the cubic spline interpolation method.

Assuming a total of (n+1) survey points have been measured, data including well depth, inclination angle, and azimuth for each of the (n+1) points have been collected.

$$\begin{cases} S_0, S_1, S_2, \cdots, S_n \\ \alpha_0, \alpha_1, \alpha_2, \cdots, \alpha_n \\ \beta_0, \beta_1, \beta_2, \cdots, \beta_n \end{cases} \tag{1}$$

In the description of wellbore trajectories, well depth is a fundamental parameter that signifies the position of the survey point. In the calculation of wellbore trajectories, well depth is used as the independent variable, while the inclination angle and azimuth are expressed as functions of well depth. According to the definition and properties of cubic spline interpolation functions, the expressions for the inclination angle function (alpha(S)) and the azimuth function (beta(S)) on the interval ([S_{k-1}, S_k]) for (k = 1, 2, ldots, n-1) are constructed.

$$\alpha(S) = \frac{M_{k-1}(S_k - S)^3}{6L_k} + \frac{M_k(S - S_{k-1})^3}{6L_k} + C_k(S_k - S) + C_{k-1}(S - S_{k-1}) \tag{2}$$

$$\beta(S) = \frac{m_{k-1}(S_k - S)^3}{6L_k} + \frac{m_k(S - S_{k-1})^3}{6L_k} + c_k(S_k - S) + c_{k-1}(S - S_{k-1}) \tag{3}$$

In the equations:

$$\begin{cases} C_k = \frac{\alpha_k}{L_k} - \frac{M_k L_k}{6}, C_{k-1} = \frac{\alpha_{k-1}}{L_k} - \frac{M_{k-1} L_k}{6} \\ c_k = \frac{\beta_k}{L_k} - \frac{M_k L_k}{6}, C_{k-1} = \frac{\beta_{k-1}}{L_k} - \frac{M_{k-1} L_k}{6} \\ M_k = \alpha''(S_k), M_{k-1} = \alpha''(S_{k-1}) \\ m_k = \beta''(S_k), m_{k-1} = \beta''(S_{k-1}) \end{cases} \tag{4}$$

The coefficients Mk and mk are obtained from the definition of the cubic spline interpolation function, which are related to the inclination angle, azimuth, and boundary conditions at the wellhead and the bottom of the well. It is assumed that the second derivatives of the inclination angle and azimuth at the wellhead and the bottom of the well are constants. Given the logging data from n+1 survey points, two sets of linear equation systems with n−1 unknowns Mk and mkmk (for k=1,2,…,n−1) can be formed.

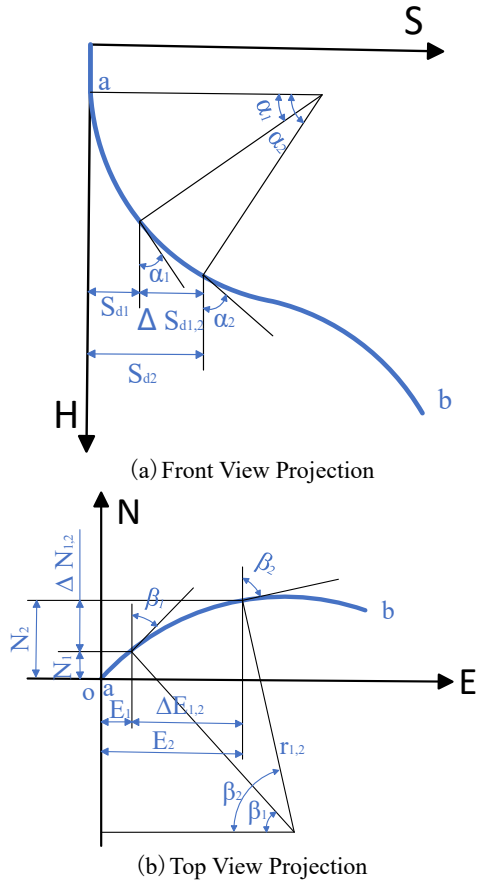
$$\begin{bmatrix} 2 & \lambda_1 & 0 & \cdots & 0 & 0 \\ \mu_1 & 2 & \lambda_2 & \cdots & 0 & 0 \\ 0 & \mu_2 & 2 & \cdots & 0 & 0 \\ \cdots & \cdots & \cdots & \cdots & \cdots & \cdots \\ 0 & 0 & 0 & \cdots & 2 & \lambda_{n-1} \\ 0 & 0 & 0 & \cdots & \mu_n & 2 \end{bmatrix} \begin{bmatrix} M_0 \\ M_1 \\ M_2 \\ \cdots \\ M_{n-1} \\ M_n \end{bmatrix} = \begin{bmatrix} D_0 \\ D_1 \\ D_2 \\ \cdots \\ D_{n-1} \\ D_n \end{bmatrix} \tag{5}$$

$$\begin{bmatrix} 2 & \lambda_1 & 0 & \cdots & 0 & 0 \\ \mu_1 & 2 & \lambda_2 & \cdots & 0 & 0 \\ 0 & \mu_2 & 2 & \cdots & 0 & 0 \\ \cdots & \cdots & \cdots & \cdots & \cdots & \cdots \\ 0 & 0 & 0 & \cdots & 2 & \lambda_{n-1} \\ 0 & 0 & 0 & \cdots & \mu_{n-1} & 2 \end{bmatrix} \begin{bmatrix} m_0 \\ m_1 \\ m_2 \\ \cdots \\ m_{n-1} \\ m_n \end{bmatrix} = \begin{bmatrix} d_0 \\ d_1 \\ d_2 \\ \cdots \\ d_{n-1} \\ d_n \end{bmatrix} \tag{6}$$

In the equations:

$$\begin{cases} D_k = \frac{6}{L_k + L_{k+1}} \left(\frac{\alpha_{k+1} - \alpha_k}{L_{k+1}} - \frac{\alpha_k - \alpha_{k-1}}{L_k} \right) \\ d_k = \frac{6}{L_k + L_{k+1}} \left(\frac{\beta_{k+1} - \beta_k}{L_{k+1}} - \frac{\beta_k - \beta_{k-1}}{L_k} \right) \\ \lambda_1 = 1, \mu_n = 0, \lambda_k = \frac{L_{k+1}}{L_k + L_{k+1}}, \mu_k = \frac{L_{k+1}}{L_k + L_{k+1}} \end{cases} \tag{7}$$

The solution to the aforementioned system of equations employs the Thomas algorithm, also known as the Thomas Algorithm. Once the coefficients (M_k) and (m_k) (for (k = 1, 2, ldots, n-1)) are determined, they are substituted into the expressions for the inclination angle function (alpha(S)) and the azimuth function (beta(S)). This allows for the calculation of the inclination angle and azimuth at any point within the interval ([S_{k-1}, S_k]) (for (k = 1, 2, ldots, n-1)).With the inclination angle and azimuth at any point along the wellbore segment, the corresponding northing and easting coordinates can be determined. By doing so, the spatial curvature of the wellbore trajectory can be ascertained, as illustrated in Figure 1.



(a) Front View Projection

(b) Top View Projection

Figure 1. Wellbore Trajectory Projection

2.2. Measurement Tool String Mechanical Analysis Model

The frictional force experienced by a tubing string is closely related to its own deflection and deformation. As the deflection of the tubing string increases, the frictional force it experiences also continues to increase. This section will provide a detailed analysis of the forces acting on the tubing string and examine the relationship between the frictional force and deflection changes during the pumping process.

When the tubing string passes through a curved section of the wellbore, the deflection of the tool string increases with the increase in wellbore curvature, and simultaneously, the frictional force between the tool string and the casing also increases. Given the known axis trajectory of the casing and casing deformation, the deflection of the tubing string can be calculated using the pass capacity condition of the tool string, and further, the action force on the midpoint of the casing, and the frictional force between the tool string and the casing can be computed.

During the pumping process of lowering the tool string, the forces on the tool string are affected by wellbore parameters of the wellbore, the density and velocity of the pumping fluid, etc. The axial component of the gravitational force on the tool string (F_p), the transverse force (F_n), the resistance force (F_f), the frictional force on the wireline(F_{f1}), and the pump thrust force (F_b) are as follows:

$$\begin{cases} F_p = WLcos\alpha \\ F_n = WLsin\alpha \\ F_f = \mu_1(WLsin\alpha + F_t) + \frac{1}{2}C_d\rho_m v_t^2 A \\ F_{f1} = W'L'sin\alpha\mu_2 \\ F_b = F_f + F_{f1} - F_p \end{cases} \tag{8}$$

In the equations: W and W' represent the buoyant weight of the tool string and wireline per unit length in the well fluid, with units of Newtons per meter (N/m). L' is the length of the wireline in the well, measured in meters (m). C_d is the drag coefficient of the fluid. v_t is the relative velocity of the tool string with respect to the well fluid, measured in meters per second (m/s). rho_m is the density of the well fluid, measured in kilograms per cubic meter (kg/\(m^3)). A is the maximum cross-sectional area of the tool string, measured in square meters (m^2).

From the analysis of the tool string pass capacity, it is known that the deformation is greatest at the midpoint of the tool string. The upper part of the tool string at the midpoint is in contact with the casing. Let (F_t) be the vertical force exerted by the casing on the axis of the tool string. When the tool string does not contact the upper wall of the casing, (F_t = 0). This leads to the force analysis diagram for the cable-conveyed tool string.

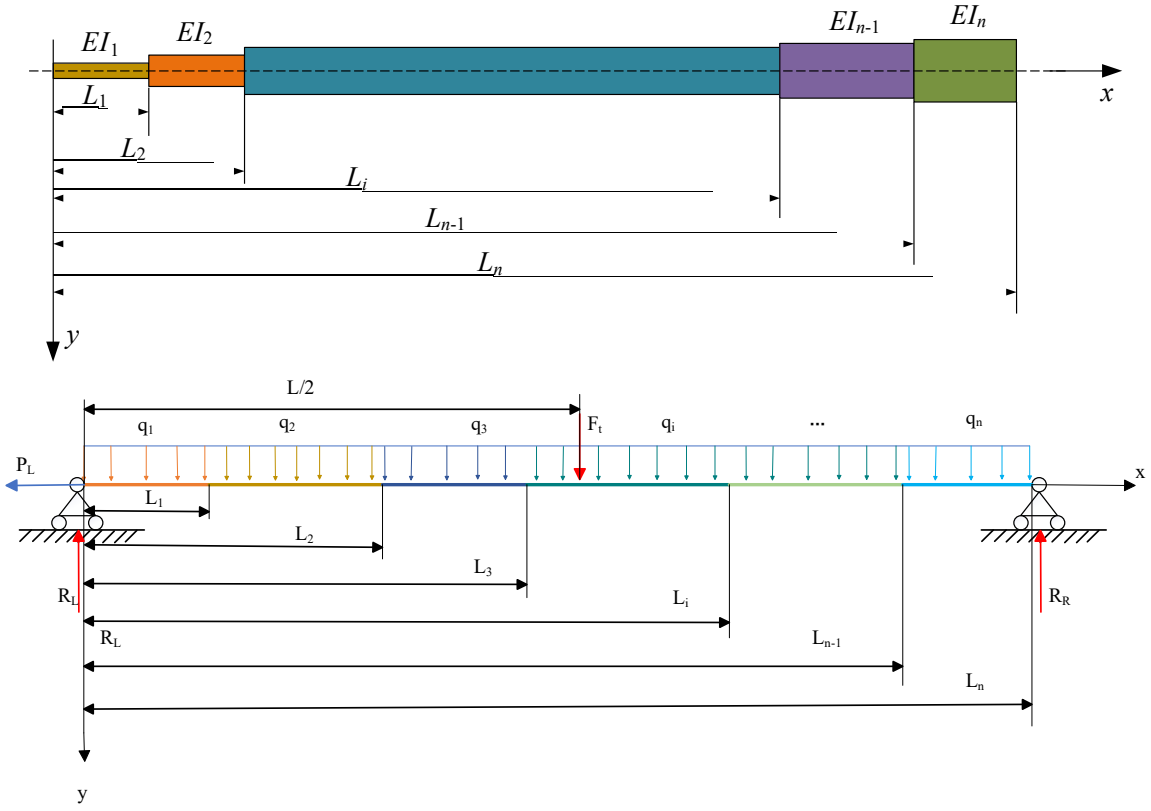


Figure 2. Wireline Pumping Tool String Force Analysis Diagram

2.3. Well Logging Tool String Throughput Model

In petroleum engineering, the pass capacity of logging tool strings is categorized into rigid pass capacity and flexible pass capacity. Rigid pass capacity refers to the scenario where the deformation of the logging tool string is not considered, while flexible pass capacity takes into account the deformation of the tool string. Practical experience in pumping operations has shown that the pass capacity calculated under rigid conditions is smaller than the actual capacity, indicating that the theory of rigid pass capacity is not sufficiently comprehensive and differs from real-world conditions. In reality, tool strings do deform within the casing, making flexible pass capacity a more accurate representation of actual conditions.

Let the wellbore curvature be denoted by (R), the casing diameter by(d_t), the outer diameter of the logging tool string at the bridge plug by (d_q), the outer diameter at the midpoint of the logging tool string by (d_m), the total length

of the tool string by L , the length after deformation by (L_r), and the deformation deflection of the tool string due to casing constraints (y_c). Based on the general pattern of drilling string pass capacity , as illustrated in the figure, we can derive the pass capacity of the drilling tool assembly.

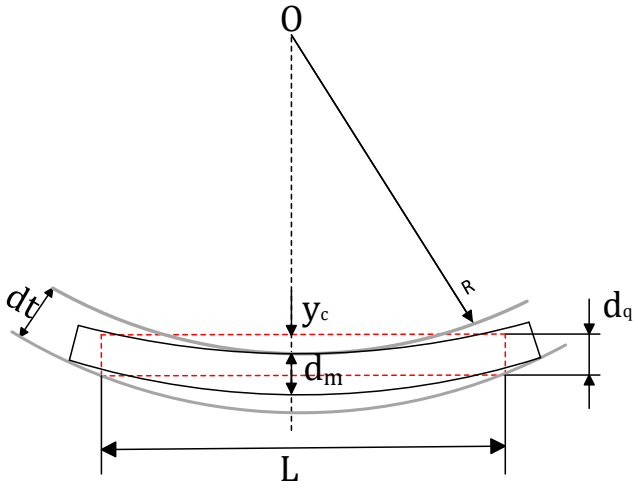


Figure 3. Well Logging Tool String Through-put Capability Analysis Chart

$$R = \frac{L^2}{8(d_z - d_b + y_c)} - \frac{d_z + d_b - y_c}{2} \quad (9)$$

$$L = 2\sqrt{(R + d_z)^2 - (R + d_b - y_c)^2} \quad (10)$$

$$y_c = R - \frac{1}{2}d_t + d_m - \sqrt{\left(R + \frac{1}{2}d_t\right)^2 - \left(\frac{L^2}{4}\right)} - \frac{1}{2}(d_q - d_m) \quad (11)$$

In actual field logging operations, it is observed that the maximum deflection y_max during the pumping process occurs at the midpoint of the tool string. Therefore, the pass capacity of the tool string can be described as follows:

If y_max >= y_c , the tool string can pass through.

If y_max <= y_c , the tool string cannot pass through.

To ensure the safe passage of the logging tool string through the casing, the following conditions must also be met:

1. Geometric Condition: The degree of bending deformation of the logging tool string during the insertion process should be less than the allowable deformation value.

2. Strength Condition: The working stress of the logging tool string (including the threaded parts) should be less than the allowable stress to prevent breakage or failure.

3. Contact Condition: The contact force between the logging tool string and the inner wall of the wellbore should be less than the allowable value, keeping the wear of the tool string within an acceptable range, and ensuring that scratches on the inner wall of the casing do not affect the operation.

These conditions are critical to ensure that the logging tool string can safely and effectively navigate through the wellbore without causing damage to the tool string or the casing, and without compromising the integrity of the well.

2.4. The Impact of Casing Deformation on the Pass Capacity of Logging Tools

Casing deformation can be categorized into compression deformation, shear deformation, and complex deformation. To analyze the impact of casing deformation on the critical deflection of the tool string, it is necessary to study compression and shear deformations separately.

When there is a change in the local internal diameter of the casing, it affects the pass capacity of the perforating tool string. With the wellbore curvature R remaining constant, if the internal diameter of the casing d_t decreases, the deflection of the perforating tool string passing through this section of the wellbore will increase. Consequently, it can be deduced from the formula that when the casing internal diameter decreases, the pass capacity of the perforating tool string in the wellbore is reduced.

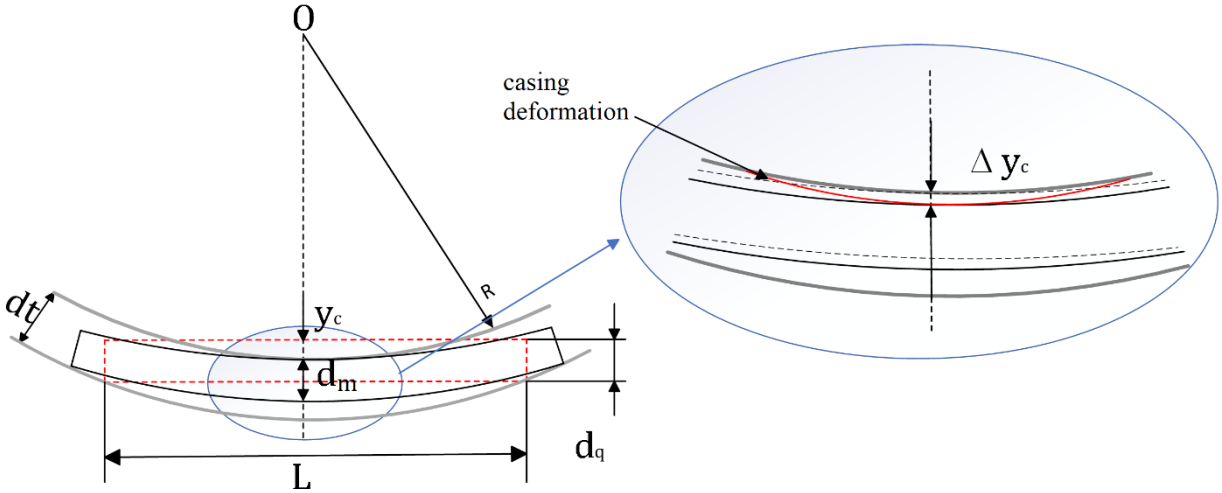


Figure 4. Tool Deflection Change Chart During Casing Deformation Due to Crushing Chart

Assuming the deformation radius of the casing is Delta d_t, in meters; since casing deformation leads to an increase in the deflection of the tool string, the calculation formula for the deflection y'_c at the maximum deformation points when the midpoint of the tool string passes through after casing deformation can be obtained.

$$y_c' = R - \frac{1}{2}(d_t - \Delta d_t) + d_m - \sqrt{[R + \frac{1}{2}(d_t - \Delta d_t)]^2 - (\frac{L^2}{4})} - \frac{1}{2}(d_q - d_m) \quad (12)$$

From the above equation, it can be concluded that in the same well section, the occurrence of compression deformation in the casing will lead to a reduction in the pass capacity of the perforating tool. The greater the dimension of the casing deformation caused by compression deformation, the larger the critical deflection produced when the same tool string passes through this well section.

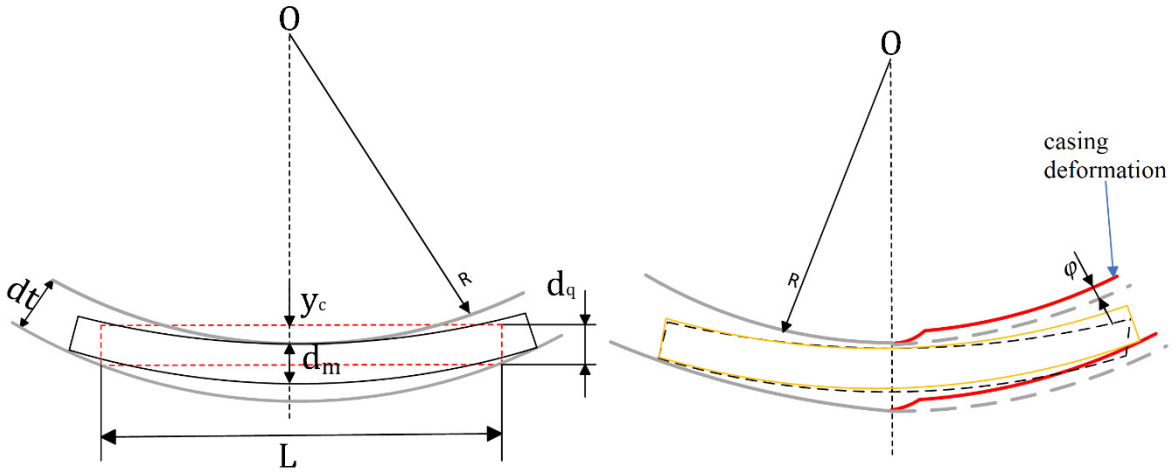


Figure 5. Tool Deflection Variation Chart During Casing Shear Deformation

In the figure, Delta represents the shear deformation of the casing, in meters.

From the analysis of the figure, it can be seen that when the casing experiences shear deformation, the critical deflection of the perforating tool string passing through the wellbore increases. Upon analysis, a formula for calculating the deflection at the midpoint of the tool string after the casing has undergone shear deformation can be derived.

$$y_c^{'} = R - \frac{1}{2}d_t + d_m - \sqrt{(R+\frac{1}{2}d_t)^2 - (\frac{L^2}{4})} - \frac{1}{2}(d_q) + \frac{1}{2}\varphi \quad (13)$$

3. Case Analysis

The main factors affecting the passability of the logging tool string include the length of the tool string, midpoint diameter, dogleg severity of the wellbore, and casing deformation. Based on the above theoretical analysis, a corresponding computer analysis program is to be developed to analyze the passability of the perforation tool combination in a horizontal well located in Southwest China. The wellbore data for this well has been provided by the logging company, including well depth, inclination angle, azimuth, and dogleg severity. The casing diameter is 0.1214 m, with a total depth of 3690 m, a maximum vertical depth of 2110.22 m, a maximum inclination angle of 91.78°, and a maximum dogleg severity of 4.89°/30 m.

Table 1. Perforating Gun and Bridge Plug String Structure Parameters

Numble	Length (m)	Outer Diameter (m)	Quantity	Individual Weight (kg)
Weak Point of Wireline	0.63	0.036	1	1.4
CCL	0.457	0.08	1	9.1
Weighted Pipe	3.325	0.0889	1	74
Ignition Head	0.29	0.0889	2	14
Perforating Gun	1.82	0.0889	2	39
Adapter Joint	0.4	0.0889	2	18.6
Bridge Plug Perforating Assembly	0.086	0.086	1	24.2
Set Bridge Plug	1.93	0.092	1	83.2
Bridge Plug	1.33	0.11	1	20
Others	2.1	0.089	1	16.5

Using the wellbore parameters and tool string parameters from the inclined section of the well, calculate the minimum deflection (yc) for the tool string in the horizontal well. Substitute the wellbore trajectory and tool string parameters into the corresponding computer program to obtain the critical deflection (yc) for the matched well section. Plot the curves of well depth versus dogleg severity and critical deflection, as shown in the figure. The analysis indicates that the critical deflection of the tool string increases with the increase in dogleg severity, meaning the maximum deflection occurs in the inclined section.

Assuming that in the well section from 1665 m to 2315 m, the casing experiences two deformations: compressive deformation at 1840 m and shear deformation at 2190 m, with deformation amounts of 3 mm and 6 mm, respectively. Substitute the casing deformation data into the corresponding well section to obtain the critical deflection of the tool string under casing deformation conditions, and plot the comparison curves of critical passable deflection for the tool string before and after casing deformation, as shown in the figure.

4. Summary

In the pumping process of complex horizontal well logging tools, the maximum critical passable deflection of the tool string occurs in the inclined section, where a greater dogleg severity results in a larger critical passable deflection. In shale gas horizontal wells, casing deformation often occurs due to factors like formation pressure and formation slippage, with common types including compressive and shear deformation.

Casing deformation increases the critical deflection required for the tool string to pass through the wellbore. This paper analyzes the impact of these two types of casing deformation on the tool string's passable deflection, incorporating actual wellbore parameters and tool string parameters to assess the effect of casing deformation on the critical deflection of the tool string.

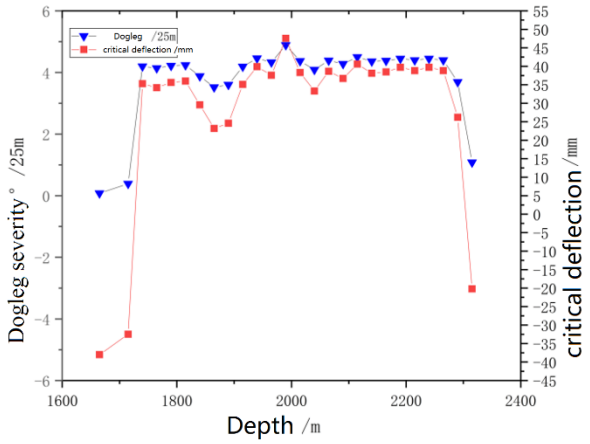


Figure 6

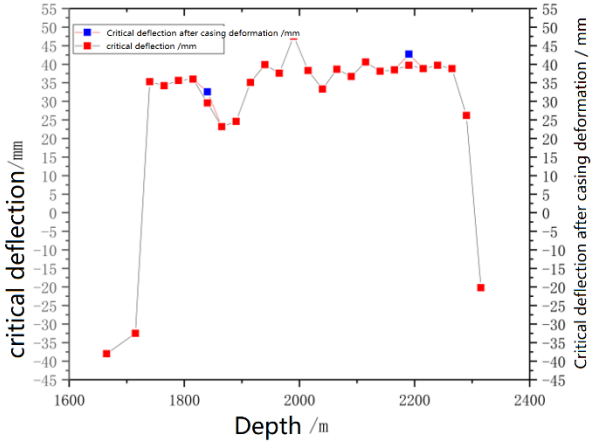


Figure 7

Figure 6. Well Depth vs. Dogleg Severity and Critical Deflection Curve Chart

Figure 7. Comparison Curve Chart of Tool String Deflection Before and After Casing Deformation

References

[1] Zhi Tianyou, "Current Status and Prospects of Shale Gas Exploration and Development Technology," Petrochemical Technology, 2020. 27(10): pp. 139-140.

[2] He Chunzeng and Cui Shasha, "Study and Application of Hydraulic Pumping Bridge Plug Segmented Fracturing Technology," Liaoning Chemical Industry, 2015. 44(2): pp. 211-213.

[3] Jin Jiangbo, "Discussion on Emergency Strategies for Pumping Bridge Plugs in Multi-stage Perforating Operations in Horizontal Wells," Journal of Jianghan Petroleum University of Staff and Workers, 2022.

[4] Liu Xueguang, Gong Yanhong, and Liu Haixia, "Experimental Application of Risk Assessment and Prevention Technology for Casing Deformation Wells," 2022. 12(6): pp. 18-21.

[5] Ran Jing, "Downhole Tools in High Inclined Well Fracturing and Acidizing," Drilling and Production Technology, 1990(02): pp. 70-73.

[6] Chen Zuxiang, Tang Xueping, and Gao Zhiqiang, "Passing Degree of Medium and Short Radius Curved Screw Drills in Casing," Drilling and Production Technology, 1999. 22(6): pp. 7-10.

[7] Zhu Xiuxing, Xue Shifeng, and Tong Xinghua, "Control Method of Pumping Parameters for Perforating and Bridge Plug Combined String in Horizontal Wells," Petroleum Exploration and Development, 2013. 40(03): pp. 371-376.

[8] Luo Quan et al., "Calculation Method and Development Trend of Downhole Tool Passing Ability," Mechanical Engineer, 2014(09): pp. 17-19.

[9] "Study on Casing Failure Mechanism," by Yang Long.

[10] Liu Wei et al., "Numerical Simulation Study on the Deformation and Failure Mechanism of Casing in Volume Fracturing of Horizontal Wells in Tight Oil Reservoirs," Bulletin of Petroleum Science, 2017. 2(4): pp. 466-477.

[11] Guo Xue Li, "Study on Load Analysis and Deformation Mechanism of Casing in Shale Gas Fracturing Wells."

[12] Chen Chaowei et al., "Casing Deformation Characteristics and Force Patterns of Sichuan Shale Gas Wells," Petroleum Machinery, 2020. 48(2): pp. 126-134.

[13] Zhao Junping and Su Yinao, "Drilling String Combination Passing Capacity Model and Its Analysis," Petroleum Drilling and Production Technology, 1993(05): pp. 1-6.

[14] Yu Fu and Shi Wei, "Analysis of Casing Deformation and Failure Causes in Shale Gas Wells," Petroleum Tubular Goods and Instruments, 2018. 4(3): pp. 35-38.